Complexes Formed in Solution Between Vanadium(IV)/(V) and the Cyclic Dihydroxamic Acid Putrebactin or Linear Suberodihydroxamic Acid

Amalie A. H. Pakchung,[†] Cho Zin Soe,[‡] Tulip Lifa,[‡] and Rachel Codd*[,†,‡]

[†]Center for Heavy Metals Research, School of Chemistry and [‡]School of Medical Sciences (Pharmacology) and Bosch Institute, University of Sydney, New South Wales 2006, Australia

Ⓢ *Supporting Information*

ABSTRACT: An aerobic solution prepared from V(IV) and the cyclic dihydroxamic acid putrebactin (pbH$_2$) in 1:1 H$_2$O/CH$_3$OH at pH = 2 turned from blue to orange and gave a signal in the positive ion electrospray ionization mass spectrometry (ESI-MS) at m/z_{obs} 437.0 attributed to the monooxoV-(V) species $[V^VO(pb)]^+$ ($[C_{16}H_{26}N_4O_7V]^+$, m/z_{calc} 437.3). A solution prepared as above gave a signal in the ^{51}V NMR spectrum at $\delta_V = -443.3$ ppm (VOCl$_3$, $\delta_V = 0$ ppm) and was electron paramagnetic resonance silent, consistent with the presence of $[V^VO(pb)]^+$. The formation of $[V^VO(pb)]^+$ was invariant of [V(IV)]:[pbH$_2$] and of pH values over pH = 2−7. In contrast, an aerobic solution prepared from V(IV) and the linear dihydroxamic acid suberodihydroxamic acid (sbhaH$_4$) in 1:1 H$_2$O/CH$_3$OH at pH values of 2, 5, or 7 gave multiple signals in the positive and negative ion ESI-MS, which were assigned to monomeric or dimeric V(V)− or V(IV)−sbhaH$_4$ complexes or mixed-valence V(V)/(IV)−sbhaH$_4$ complexes. The complexity of the V-sbhaH$_4$ system has been attributed to dimerization ($2[V^VO(sbhaH_2)]^+ \leftrightarrow [(V^VO)_2(sbhaH_2)_2]^{2+}$), deprotonation ($[V^VO(sbhaH_2)]^+ - H^+ \leftrightarrow [V^VO(sbhaH)]^0$), and oxidation ($[V^{IV}O(sbhaH_2)]^0 - e^- \leftrightarrow [V^VO(sbhaH_2)]^+$) phenomena and could be described as the sum of two pH-dependent vectors, the first comprising the deprotonation of hydroxamate (low pH) to hydroximate (high pH) and the second comprising the oxidation of V(IV) (low pH) to V(V) (high pH). Macrocyclic pbH$_2$ was preorganized to form $[V^VO(pb)]^+$, which would provide an entropy-based increase in its thermodynamic stability compared to V(V)−sbhaH$_4$ complexes. The half-wave potentials from solutions of [V(IV)]:[pbH$_2$] (1:1) or [V(IV)]:[sbhaH$_4$] (1:2) at pH = 2 were $E_{1/2}$ −335 or −352 mV, respectively, which differed from the expected trend ($E_{1/2}$ [VO(pb)]$^{+/0}$ < V$^{V/IV}$−sbhaH$_4$). The complex solution speciation of the V(V)/(IV)−sbhaH$_4$ system prevented the determination of half-wave potentials for single species. The characterization of $[V^VO(pb)]^+$ expands the small family of documented V−siderophore complexes relevant to understanding V transport and assimilation in the biosphere.

■ INTRODUCTION

The ability of microbial siderophores to coordinate metal ions, particularly Fe(III), continues to generate interest in the potential applications of these bioligands in the environment and medicine.[1−3] Siderophores produced by terrestrial and marine bacteria have evolved to sequester Fe(III) from insoluble Fe(III)-oxy/hydroxides under oxic and pH neutral environments.[4−7] The formation of the Fe(III)−siderophore complex is the first step in siderophore-dependent iron uptake and is essential for the viable growth of almost all environmental and pathogenic bacteria.[8−12] Siderophores have diverse structures and have been classified according to the metal ion-binding functional group as catechol-, hydroxamic acid- or citric acid-based compounds.[13] Clinical applications of hydroxamic acid-based siderophores include the mesylate salt of desferrioxamine B for the treatment of iron-overload disease in patients undergoing frequent blood transfusions and suberoylanilide hydroxamic acid, which acts as an anticancer agent via the inhibition of Zn(II) containing histone deacetylases.[14−18]

While siderophores have evolved as high-affinity Fe(III) complexing agents, these ligands have a rich coordination chemistry with other transition-metal ions in the first and second row of the Periodic Table.[19] Siderophores excreted by marine bacteria compete for Fe(III) and other transition-metal ions present in greater abundance in the ocean, such as Mo(VI) and V(V).[20] Nitrogen fixing *Azotobacter vinelandii* produces a suite of siderophores that bind Fe(III) and V in order to meet its V requirement for the biosynthesis of V-containing nitrogenase.[21] Desferrioxamine B reactivated V(V)-inhibited enzymes by sequestering the V(V) ion at the active site[22] and the V(V)-hydroxamic acid complexes inhibited the β-lactamase of *Enterobacter cloacae* P99.[23] Complexes between V(IV) or V(V) and hydroxamic acids lowered blood glucose levels in rat adipocytes[24] and streptozotocin-induced diabetic mice[25] and are under

Chart 1. Putrebactin (pbH$_2$, 1) and Suberodihydroxamic Acid (sbhaH$_4$, 2)
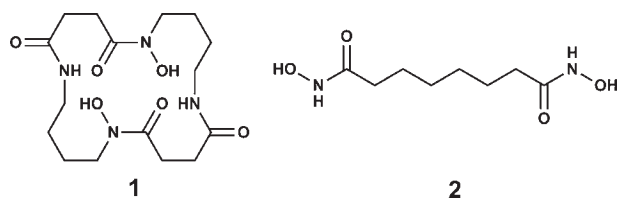
increasing scrutiny as antidiabetic agents. Despite the importance of the coordination chemistry of V and siderophores, there have been few complexes characterized. The triscatecholate-based siderophore enterobactin formed an unusual desoxoV(IV) complex that has been characterized by X-ray crystallography,[26,27] and complexes between desferrioxamine B and V(V) have been characterized in solution.[28]

The cyclic dihydroxamic acid-based siderophore putrebactin (pbH$_2$, 1, Chart 1) is a 20-membered macrocycle produced by *Shewanella putrefaciens*.[29−31] The cyclic dihydroxamic acid-based class of siderophores features only two other members: alcaligin produced by pathogenic *Bordetella pertussis* and *B. parapertussis* and bisucaberin produced by *Alteromonas haloplanktis* and *Aliivibrio salmonicida*.[32−35] It was shown by the group that first discovered and fully characterized pbH$_2$ that the Fe(III):pbH$_2$ stoichiometry changed from 1:1 at pH = 2 to 2:3 at pH = 6, with the 6 coordination sites of each of the 2 Fe(III) centers in the latter complex fully saturated by 3 tetradentate pb(2−) ligands.[29] This was similar to the 2:3 complex characterized in solution and in the solid state between Fe(III) and alcaligin[33,36] or between Fe(III) and the linear dihydroxamic acid rhodotorulic acid.[37,38] Due to the low yields produced in culture and the complex nature of the total syntheses of cyclic dihydroxamic acids,[39,40] the coordination chemistry of pbH$_2$ has not been studied beyond Fe(III). Since pbH$_2$ has four hydroxamic acid-derived oxygen donor atoms positioned within a constrained macrocycle, we predicted that pbH$_2$ would form stable mononuclear complexes with oxoV(IV) or oxoV(V) centers, with the oxo group in a five-coordinate species positioned above the metal−ligand plane. This posit was supported by the results from studies of the coordination chemistry of V(V) or Cr(V) and abiological hydroxamic acids.[41,42] With limited amounts of native pbH$_2$ available from culture, we have characterized species formed in solution between V(V)/(IV) and pbH$_2$ using electronic absorption spectroscopy, electrospray ionization mass spectrometry (ESI-MS), ^{51}V NMR spectroscopy, electron paramagnetic resonance (EPR) spectroscopy and cyclic voltammetry. To gain insight into the differences in speciation between V(V)/(IV) and cyclic or linear dihydroxamic acids, experiments using the linear dihydroxamic acid suberodihydroxamic acid (sbhaH$_4$, 2, Chart 1) were conducted in parallel.

Mapping the species formed from solutions of V(V)/(IV) and a difficult-to-access cyclic dihydroxamic acid-based siderophore native to a bacterial species of *Shewanella* has implications for a better understanding of V(V)/(IV)-siderophore chemistry in marine environments.

■ EXPERIMENTAL SECTION

Chemicals and Bacterial Strain. All reagents were obtained from commercial sources and used without further purification.

Suberodihydroxamic acid (sbhaH$_4$) and NaVO$_3$ were purchased from Sigma-Aldrich Co. VOSO$_4$·5H$_2$O was obtained from Merck. *S. putrefaciens* 8071^T was obtained from the American Type Culture Collection (ATCC). Methanol and acetonitrile were HPLC grade from LabScan. Milli-Q water (18.2 Ω) was used in all experiments. The pH values of the solutions were adjusted with 0.1 M NH$_4$OH, 0.1 M NaOH, or 0.1 M HCl, as stipulated. As measured for each solution at t = 15 min after preparation and at t = 1 h after analysis, the change in the pH value in all experiments was <0.1 pH unit.

Instrumentation. ESI-MS was carried out using a Finnigan LCQ mass spectrometer (San Jose, CA) in both positive and negative ion modes. The mobile phase was methanol, with a flow rate = 0.20 mL min^{-1}, cone voltage was 25 V, and the injection volume was 20 μL. Electronic absorption spectra were acquired with a Cary 1E UV−vis spectrophotometer. ^{1}H NMR spectra were recorded on a 300 MHz Bruker Avance300 NMR spectrometer at 300 K. ^{51}V NMR spectra were recorded at 105 MHz on a 400 MHz Bruker DPX400 NMR spectrometer using a capillary VOCl$_3$ reference (0 ppm). EPR spectra were acquired using a Bruker Elexsys 500 spectrometer at 150 K under the following conditions: Center field, 3330 G; sweep width, 2000 G; resolution, 1024; modulation frequency, 100 kHz; modulation amplitude, 2 G; time constant, 1.28 ms; conversion time, 40.96 ms; microwave power, 6.241 mW; microwave frequency, 9.3470 GHz; and no. of scans, 20. Cyclic voltammetry experiments were carried out using a Bioanalytical Systems BAS 100B Electrochemical Analyzer (scan rate, 100 mV s^{-1}), 100% iR compensation) with a Pt working electrode, a Ag/AgCl reference electrode, and Pt wire as an auxiliary electrode. Samples were degassed with Ar for 10 min prior to data acquisition.

Purification of pbH$_2$ from *S. putrefaciens* 8071^T. The culture supernatant of two large-scale, Fe(III)-deficient cultures of *S. putrefaciens* 8071^T (30 and 50 L culture medium) were purified as previously described.[29,43] The pbH$_2$ obtained from the 30-L culture (26.6 mg) was dissolved in an aliquot (~7 mL) 1:1 CH$_3$OH/H$_2$O at pH = 2 (~10.2 mM, Batch 1), and the pbH$_2$ obtained from the 50-L culture (64.4 mg) was dissolved in an aliquot (17.2 mL) of 1:1 CH$_3$OH/H$_2$O at pH = 2 (~10 mM, Batch 2). Based on RP-HPLC and ^{1}H NMR spectroscopic measurements, Batch 1 was ~50% pure and Batch 2 was ~40% pure. Some experiments used a solution of pbH$_2$ (~11 μM in 40:60 CH$_3$OH/H$_2$O, pH = 2) that had not been purified by RP-HPLC (Batch 3).

Solution Preparation: Electronic Absorption Spectroscopy and ESI-MS. Solid VOSO$_4$·5H$_2$O (0.03 g, 0.12 mmol) was added to an aliquot of pbH$_2$ (2 mL, ~20 μmol, Batch 1) to give a V(IV):pbH$_2$ solution in a ~6:1 ratio at pH = 2. The resulting purple/red solution was stirred at room temperature. After standing overnight at room temperature, the solution was subjected to ESI-MS (positive ion mode) and an electronic absorption spectrum was obtained (300−900 nm). The solution was stored in a closed vial at room temperature for 15 months, and the positive ion ESI-MS was reacquired after this time. An aliquot of an aqueous solution of VOSO$_4$·5H$_2$O (200 μL, 1 mM) was added to an aliquot of pbH$_2$ (100 μL, Batch 3), and the solution was monitored by electronic absorption spectroscopy (300−900 nm) every 2 min over 90 min and again at 24 h. An aliquot of an aqueous solution of NaVO$_3$ (30 μL, 1 mM) was added to an aliquot of pbH$_2$ (750 μL of Batch 3) to give a V(V):pbH$_2$ solution in approximately a 3.5:1 ratio, and the pH value was adjusted to pH = 2. After stirring at room temperature overnight, the yellow/orange solution was analyzed by positive and negative ion ESI-MS. An aliquot of an aqueous solution of VOSO$_4$·5H$_2$O (200 μL, 1 mM) was added to an aliquot of pbH$_2$ (100 μL, Batch 3), the pH value of the solution was adjusted to pH = 2, and the solution was analyzed by negative ion ESI-MS. An aliquot of an aqueous solution of VOSO$_4$·5 H$_2$O (4 mL, 10 mM) was added to an aliquot of pbH$_2$ (4 mL, Batch 2), and the orange solution was stirred at room temperature. After standing overnight at room temperature, the solution was lyophilized to yield a

5979

dx.doi.org/10.1021/ic1025119 |*Inorg. Chem.* 2011, 50, 5978–5989

solid purple residue. The purple solid was dissolved in methanol (1 mL) to give an orange solution, which was applied to a Sephadex LH-20 column (16 × 1.2 cm i.d., CV = 18.1 cm^3) which was eluted with CH$_3$OH (flow rate ~0.5 mL min^{-1}). An orange band eluted at 10 mL, and a yellow band eluted at 25 mL. Both fractions were collected and analyzed by positive and negative ion ESI-MS. Solutions of VOSO$_4$·5 H$_2$O (1 mM stock solution in 10 mM HCl) and pbH$_2$ were prepared in which [V(IV)]:[pbH$_2$] = 1:1 (pH = 2); 1:1.5 (pH = 2 or 7); 1:2 (pH = 7) and were analyzed by positive and negative ion ESI-MS and by electronic absorption spectroscopy.

An aliquot of an solution of VOSO$_4$·5H$_2$O in 0.1 M HCl (1 mL, 10 mM) was added to an aliquot of sbhaH$_4$ (2 mL, 10 mM) in 1:1 CH$_3$OH:H$_2$O and the pH value of the solution was adjusted to pH = 2 with 0.1 M HCl. Three additional solutions were prepared at pH = 5, 7, and 9. Each solution was analyzed by positive ion and negative ion ESI-MS and by electronic absorption spectroscopy.

Solution Preparation: ^{51}Vanadium NMR Spectroscopy. An aliquot of an aqueous solution of VOSO$_4$·5H$_2$O (0.4 mL, 10 μM) was added to an aliquot of pbH$_2$ (0.4 mL, 10 μM, Batch 2), and the orange solution (pH = 2) was left to stand overnight at room temperature. The solution was lyophilized to dryness, and the residue was dissolved in methanol (~1 mL) before passing the solution through a Sephadex LH-20 column, as described above. The orange band was collected, the solution was lyophilized, and the residue was dissolved in CD$_3$OD (0.5 mL) for analysis by ^{51}V NMR spectroscopy. An aliquot of a D$_2$O solution of VOSO$_4$·5H$_2$O (0.167 mL, 2 mM) was added to an aliquot (0.333 mL, 2 mM) of sbhaH$_4$ in D$_2$O, and the pH value of the solution was adjusted to pH = 2 using 0.1 M HCl (5 μL of 10.17 M HCl in 5 mL D$_2$O). Two additional V(IV):sbhaH$_4$ = 1:2 solutions were prepared at pH = 5 or 7, with the pH values of the solutions adjusted using 0.1 M NaOH (20 mg NaOH in 5 mL D$_2$O).

Solution Preparation: EPR Spectroscopy. Methanol stock solutions of: VOSO$_4$·5H$_2$O at 10 mM (0.063 g in 25 mL) or 1 mM (0.0063 g in 25 mL) or sbhaH$_4$ at 10 mM (0.0511 g in 25 mL) were prepared. An aliquot of a methanol solution of VOSO$_4$·5H$_2$O (5 μL, 1 mM) was added to an aliquot of pbH$_2$ (900 μL, ~11 μM, Batch 3) to give an approximately V:pbH$_2$ = 1:2 solution. The solution was purified by Sephadex LH-20 column chromatography, as described above, and the orange band was subject to EPR analysis at 150 K. An aliquot of a methanol solution of VOSO$_4$·5H$_2$O (1 mL, 10 mM) was added to a methanol solution of sbhaH$_4$ (2 mL, 10 mM), and the pH value of the solution was adjusted with 0.1 M HCl to pH = 2. The solution was left at room temperature for 15 min prior to EPR analysis at 150 K. A second V(IV):sbhaH$_4$ = 1:2 solution was prepared as above, and the pH value was adjusted to pH = 5 with 0.1 M NH$_4$OH.

Solution Preparation: Electrochemistry. An aliquot (1 mL) of an aqueous solution of VOSO$_4$ (10 mM) was added to ~25 μmol pbH$_2$, and the orange solution was passed through an LH-20 column as described above, and was eluted with methanol. The orange band was collected, and the methanol was removed to yield 10.5 mg of purple solid which was dissolved in 5 mL of 0.1 M NaCl. The pH value of the solution was adjusted to pH = 2. An aliquot (2 mL) of sbhaH$_4$ (10 mM in 0.1 M NaCl) was added to an aliquot (1 mL) of VOSO$_4$ (10 mM in 0.1 M NaCl). The volume was made to 6 mL with 0.1 M NaCl solution to give a final solution of [V(IV)]:[sbhaH$_2$] = 1.67 mM:3.33 mM, and the pH value of the solution was adjusted to pH = 2.

■ RESULTS AND DISCUSSION

Rationale. In this study, the coordination chemistry of V(IV) and cyclic pbH$_2$ or linear sbhaH$_4$ has been explored. Due to the limited yields of pbH$_2$ obtained from iron-limited cultures of *S. putrefaciens*, the coordination chemistry of pbH$_2$ has not been studied beyond Fe(III).[29] The configuration of the oxygen donor
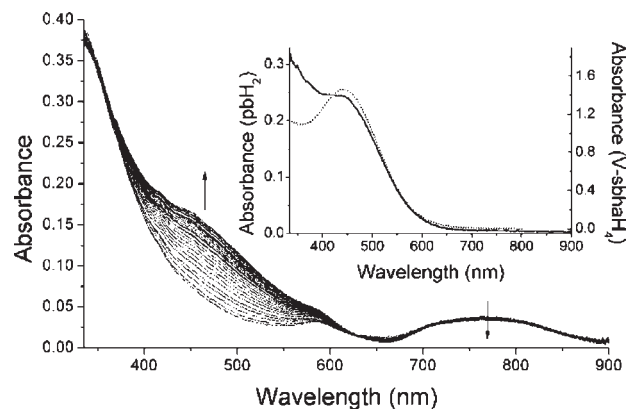

Figure 1. Electronic absorption spectra from an aqueous solution of VOSO$_4$·5H$_2$O (1 mM) and pbH$_2$ (<1 mM) acquired over 2 min intervals for 90 min. The inset shows the electronic absorption spectra from an aqueous 1:2 solution of V(IV) and shbaH$_4$ (pH = 5, dashed line) or an aqueous 1:1 solution of V(IV) and pbH$_2$ (pH = 2, solid line).

atoms of pbH$_2$ suggested that this ligand would form stable complexes with oxoV(IV) or oxoV(V) which is of interest in the context of siderophores in the marine environment, particularly given that many species of *Shewanella* are marine bacteria[44] and that in seawater V is present at 20–35 pM and is second to Mo as the most abundant transition metal.[20,45] This work has mapped solution species formed between V(IV) and pbH$_2$ or sbhaH$_4$ using electronic absorption spectroscopy, positive and negative ion mode ESI-MS, ^{51}V NMR spectroscopy, EPR spectroscopy, and cyclic voltammetry.

Electronic Absorption Spectroscopy. The solution formed from mixing V(IV) with pbH$_2$ (1:1 CH$_3$OH/H$_2$O at pH = 2) in an approximate 6:1 ratio was initially blue in color. After stirring for 1 h, the solution became dark-purple/red in color and gave an electronic absorption spectrum with λ_{max} at 452 and 760 nm. Hydroxamic acids are known to form highly colored complexes with V, which has been used for the analytical detection of submillimolar amounts of V.[46,47] A time-course study with [V(IV)] > [pbH$_2$] showed that the distribution of species formed between V and pbH$_2$ reached equilibrium at t = 90 min, with the spectrum acquired at 24 h similar to that at t = 90 min (Figure 1). There were two isosbestic points at 354 and 630 nm, indicating the presence of at least two species in solution. One of these species was VOSO$_4$, as indicated by the peak at 760 nm. The peak at 452 nm compared well with the electronic absorption spectra of previously characterized V(V)−hydroxamato complexes in CH$_3$OH/H$_2$O solutions[41] and was similar to the spectrum from a red solution prepared from V(IV) and sbhaH$_4$ (λ_{max} = 444 nm, Figure 1 inset, dashed line) in which the V(IV) had been oxidized to V(V). The electronic spectrum from a solution prepared from V(IV) and pbH$_2$, where [pbH$_2$] > [V(IV)] (Figure 1 inset, solid line) was similar to that of the V(V)-sbhaH$_4$ spectrum, which suggested that a solution of V(IV) and pbH$_2$ yielded V(V)-pbH$_2$ species.

ESI-MS from Solutions of V(IV) or V(V) and pbH$_2$. The ESI-MS (positive ion) spectrum from the ~6:1 V(IV):pbH$_2$ solution at pH = 2 gave a major signal at m/z 437.0 (100%, Figure 2a), which formulated as the V(V) species [V^{V}O(pb)]$^+$ ([C$_{16}$H$_{26}$N$_4$-O$_7$V]$^+$, m/z_{calc} 437.3) in which pb(2−) coordinates in a tetradentate fashion to a monooxoV(V) center to give a five-coordinate species (Scheme 1, **3**). A model of [V^{V}O(pb)]$^+$ built
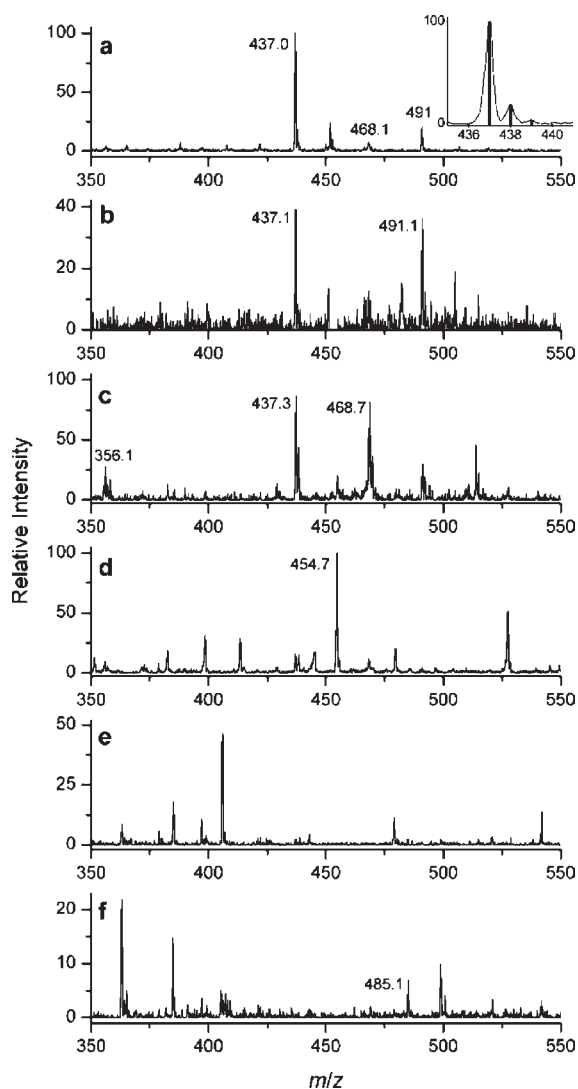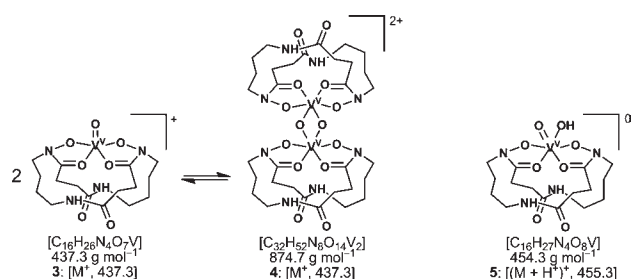
Figure 2. Positive ion ESI-MS spectra from 1:1 H$_2$O:CH$_3$OH solutions at pH = 2 of: (a) V(IV):pbH$_2$ ~6:1; (b) V(V):pbH$_2$ = ~3.5:1; (c) V(IV):pbH$_2$ ~1:1 after purification by Sephadex LH-20; and (d) V(IV):pbH$_2$ ~6:1 after 15 months aging. Negative ion ESI-MS spectra from 1:1 H$_2$O:CH$_3$OH solutions at pH = 2 of: (e) V(IV):pbH$_2$ ~1:1 and (f) V(V):pbH$_2$ ~1:1.

Scheme 1. Structures of $[V^VO(pb)]^+$ (3), $[(V^VO)_2(pb)_2]^{2+}$ (4), and $[V^VO(OH)(pb)]$ (5)

using HyperChem 7.5 from X-ray crystal structure data of Fe$_2$(alcaligin)$_3$[36] and bis(thiomaltolato)oxoV(IV)[48] shows pb-(2−) forming a bucket-type structure below the V(V) ion, which,
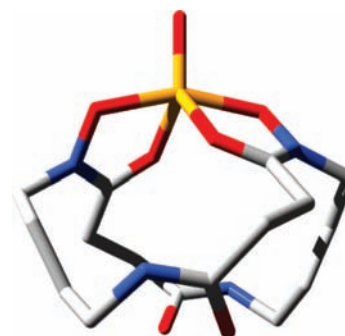

Figure 3. Predicted structure of $[V^VO(pb)]^+$ based upon the X-ray crystal structure of Fe$_2$(alcaligin)$_3$.[36] H atoms have been omitted for clarity.

similar to Fe(III)-alcaligin, lifts the metal ion out of the plane (Figure 3). This structure would be expected to prevent other ligands coordinating trans to the oxo group.[41] An additional methanol, hydroxyl or water ligand would give a six-coordinate complex, such as $[V^VO(OH)(pb)]$, with the ancillary ligand cis to the oxo group.

The ESI-MS signal simulated well as $[V^VO(pb)]^+$ (Figure 2a, inset). This species may be in equilibrium with the dimeric species $[(V^VO)_2(pb)_2]^{2+}$ ($[C_{32}H_{52}N_8O_{14}V_2]^{2+}$, m/z_{calc} 437.3) where two oxo groups bridge the two V(V) centers to form a hexacoordinate bis(μ-oxo) complex (4, Scheme 1). Compressed ESI-MS isotope patterns can be used to differentiate between mononuclear and dimeric coordination complexes with hydroxamic acid in cases where the metal ion, such as Fe(III) or Ga(III), is polyisotopic.[49] Since V is monoisotopic (natural abundance [51]V, 99.75%), the nuclearity of complexes will not be reflected in compressed ESI-MS isotope patterns. Therefore, signals due to $[V^VO(pb)]^+$ and $[(V^VO)_2(pb)_2]^{2+}$ would be indistinguishable at the level of ESI-MS. Signals in the ESI-MS at m/z_{obs} 468.1 (7%) and 491.0 (21%) were attributed to $[V^VO(pb)(CH_3OH)]^+$ (m/z_{calc} 469.4) and the Na$^+$ adduct of $[V^VO(pb)(OCH_3)]$ (m/z_{calc} 491.4), respectively. Signals corresponding to pbH$_2$ ($[M + H]^+$ m/z_{calc} 373.2) or its adducts were not observed. The presence of the intrinsically uncharged V(IV) complex $[V^{IV}O(pb)]$ is discounted since the $[M + H^+]^+$ adduct of this species would be expected to give a signal in the positive ion ESI-MS centered at m/z_{obs} 438.4, which was not the case. The orange/red color of the solution, the electronic absorption spectrum and the ESI-MS data supported the formation of $[V^VO(pb)]^+$ from solutions of V(IV) and pbH$_2$. Previous work has established the formation of V(V)−hydroxamic acid complexes from V(IV) and described the orange color of methanol solutions of these complexes and the violet color of methanol free residues.[41,47,50] This was similar to the physical characteristics of the $[V^VO(pb)]^+$ system. If $[V^VO(pb)]^+$ was being formed from a solution of V(IV) and pbH$_2$, then the ESI-MS from this solution would be expected to be similar to that from a solution of V(V) and pbH$_2$, where no redox chemistry was taking place. A dilute solution of NaVO$_3$ and pbH$_2$ gave a signal in the ESI-MS (positive ion) at m/z_{obs} 437.1 (Figure 2b) with other signals at m/z values similar to those observed for the solution prepared from V(IV) and pbH$_2$. The relative concentration of the signal at m/z_{obs} 437.0 in the ESI-MS ascribed to $[V^VO(pb)]^+$ was largely invariant of pH value and of the [V(IV)]:[pbH$_2$] ratio (Table 1). This contrasts with the Fe(III)-pbH$_2$ or -alcaligin systems, which

Table 1. Positive and negative ion mode ESI-MS data from 1:2 solutions of V(IV) and pbH$_2$ or sbhaH$_4$ at pH = 2, 5 or 7

species	no.	m/z_{calc}[b]	pH 2 m/z_{obs} (%)	pH 5 m/z_{obs} (%)	pH 7[a] m/z_{obs} (%)
$[V^VO(pb)]^{+c}$	3, 4	437.3	436.9 (100)	NC^d	437.1 (100)
$[V^VO(OH)(pb)]^e$	5	455.3	454.7 (100)^f		
$[sbhaH_4]^e$	2	205.2	ND^g	ND	204.7 (38)
$[sbhaH_3]^-$	2	203.2	ND	ND	203 (29)
$[sbhaH_3 \cdot sbhaH_4]^-$	2	407.4	ND	ND	407 (10)
$[V^VO(sbhaH_2)]^+$, $[(V^VO)_2(sbhaH_2)_2]^{2+}$	6, 12	269.1	268.7 (7)	268.7 (4)	268.8 (3)
$[V^VO(sbhaH_2)(CH_3OH)]^+$, $[(V^VO)_2(sbhaH_2)_2(CH_3OH)_2]^{2+}$	6·M, 12·M	301.1	300.4 (100)	300.5 (100)	300.5 (100)
$[V^VO(sbha)]^-$, $[(V^VO)_2(sbha)_2]^{2-}$	10, 24	267.1	266.6 (3)	266.9 (6)	267 (47)
$[V^VO(sbha)(CH_3OH)]^-$, $[(V^VO)_2(sbha)_2(CH_3OH)_2]^{2-}$	10·M, 24·M	299.2	ND	ND	300.8 (20)
$[(V^{IV}O)(V^VO)(sbhaH_2)_2]^+$	14	538.2	537.5 (6)	537.8 (5)	537.9 (5)
$[(V^VO)_2(sbhaH_2)(sbhaH)]^+$	15	537.3	ND	536.9 (6)	536.9 (12)
$[(V^VO)_2(sbhaH_2)(sbhaH)(CH_3OH)]^+$	15·M	569.3	ND	568.8 (12)	568.8 (20)
$[(V^{IV}O)_2(sbhaH_2)(sbhaH)(CH_3OH)]^-$	16·M	569.3	569.8 (47)	ND	ND
$[V^{IV}O(sbhaH)(CH_3OH)]^-$, $[(V^{IV}O)_2(sbhaH)_2(CH_3OH)_2]^{2-}$	9·M, 19·M	300.1	300.6 (90)	ND	ND
$[(V^{IV}O)(V^VO)(sbhaH)_2(CH_3OH)]^-$	20·M	569.3	568.7 (42)	ND	ND
$[(V^VO)_2(sbhaH)(sbha)]^-$	21	535.3	ND	534.9 (6)	534.9 (42)
$[(V^VO)_2(sbhaH)(sbha)(CH_3OH)]^-$	21·M	568.3	ND	ND	568.9 (20)

^{a} Spectra acquired at pH = 9 were similar to those at pH = 7. ^{b} m/z_{calc} for M$^+$ or M$^-$ ion, unless otherwise specified. ^{c} The metal:pbH$_2$ ratio was 1:1.5 at pH = 2. ^{d} NC is not acquired. ^{e} m/z_{calc} for $[M + H^+]^+$. ^{f} Aged solution. ^{g} ND is not detected.

show a pH-dependent distribution of complexes of different stoichiometries.[29,33,36,38]

One orange and one yellow band were resolved using LH-20 size exclusion chromatography from a methanol solution prepared from V(IV) and pbH$_2$. The orange fraction analyzed in the positive ion ESI-MS as $[V^VO(pb)]^+$ (m/z_{obs} 437.3) (Figure 2c). As a result of the methanol-based chromatographic procedure the intensity of the signal ascribed to $[V^VO(pb)(CH_3OH)]^+$ in this solution (m/z_{obs} 468.7) was similar to the intensity of the signal for $[V^VO(pb)]^+$. The complex signals between m/z_{obs} 356.1 to 358.1 could be ascribed to an pbH$_2$ adduct with one hydroxamic acid group reduced to an amine ($C_{16}H_{29}N_4O_5$, $[M + H^+]^+$ m/z_{calc} 357.4). The positive ion ESI-MS from the yellow fraction contained no free pbH$_2$ and was likely to contain polyoxovanadates.

The solution of V-pbH$_2$ that had been stored at room temperature for 15 months, gave rise to a signal at m/z_{obs} 454.7 (100%) (Figure 2d), which was consistent with the six-coordinate species $[V^VO(OH)(pb)]$ ($[M + H^+]^+$, m/z_{calc} 455.3) in which a hydroxide ligand has coordinated to $[V^VO(pb)]^+$ (**5**, Scheme 1). The time period over which $[V^VO(OH)(pb)]$ formed was not clear, since ESI-MS spectra were acquired from solutions of V(IV) and pbH$_2$ that were aged for <1 d and 15 months but not in between these times. Attempts to isolate the $CF_3SO_2^-$ salt of $[V^VO(pb)]^+$ and to bind $[V^VO(pb)]^+$ to a cation-exchange resin from 1 to 2 day-old solutions of V(IV) and pbH$_2$ were unsuccessful, which indicates that the concentration of $[V^VO(OH)(pb)]$ may be significant over time periods <15 months.

The presence of six-coordinate $[V^VO(OH)(pb)]$ suggested that *cis*-dioxoV(V)-pbH$_2$ species, such as $[V^VO_2(pb)]^-$, might be present. None of the signals in the negative ion ESI-MS from a solution of V(IV) and pbH$_2$ were ascribable to *cis*-dioxoV(V)-

pbH$_2$ species (Figure 2e). The signal at m/z 485.1 in the negative ion ESI-MS from a solution of V(V) and pbH$_2$ could be ascribed to the methanol adduct $[V^VO_2(pb)]^- \cdot CH_3OH$ (m/z_{calc} 485.4) (Figure 2f). The relative concentration of this species is low (7%). The remaining signals in the negative ion spectrum are attributed to background ions or impurities in pbH$_2$.

ESI-MS from Solutions of V(IV) and sbhaH$_4$: Opening Comments. Spectra were acquired from 1:2 solutions of V(IV):sbhaH$_4$ at pH = 2, 5, 7 (Figure 4), and 9 and from a 1:1 solution of V(IV):sbhaH$_4$ at pH = 2 (Table S1, Supporting Information). Compared to pbH$_2$, more signals were present in spectra from solutions of V(IV) and sbhaH$_4$, which suggested a more complex speciation profile. This increased complexity was made more acute by the fact that sbhaH$_4$ was pure and that signals were not attributable to ligand impurities. Based on previous work, it was reasonable to expect that dihydroxamate or dihydroximate complexes would predominate at low or high pH values, respectively.[51−56] The former complexes would more likely be detected by positive ion mode ESI-MS and the latter complexes by negative ion mode. Mixed hydroxamate/hydroximate complexes might form at intermediate pH values, some of which could be intrinsically uncharged and MS-inactive. Further, since the V(IV) ion is more acid stable than the V(V) ion, it was reasonable to expect that at pH = 2, [V(IV)-sbhaH$_4$] > [V(V)-sbhaH$_4$] and at pH = 7 [V(V)-sbhaH$_4$] > [V(IV)-sbhaH$_4$]. This was borne out from the results of the ^{51}V NMR and EPR spectroscopy experiments (discussed further below).

In the negative ion ESI-MS data there was a discontinuity in the signals observed from solutions at pH = 5, compared to pH = 2 and 7. The major signal at m/z_{obs} 300.6 present in the spectrum at pH = 2 and m/z_{obs} 300.8 at pH = 7 (Figure 4 panels d and f, respectively) was absent in the spectrum at pH = 5 (Figure 4, panel e). This suggested that MS-active species were present in
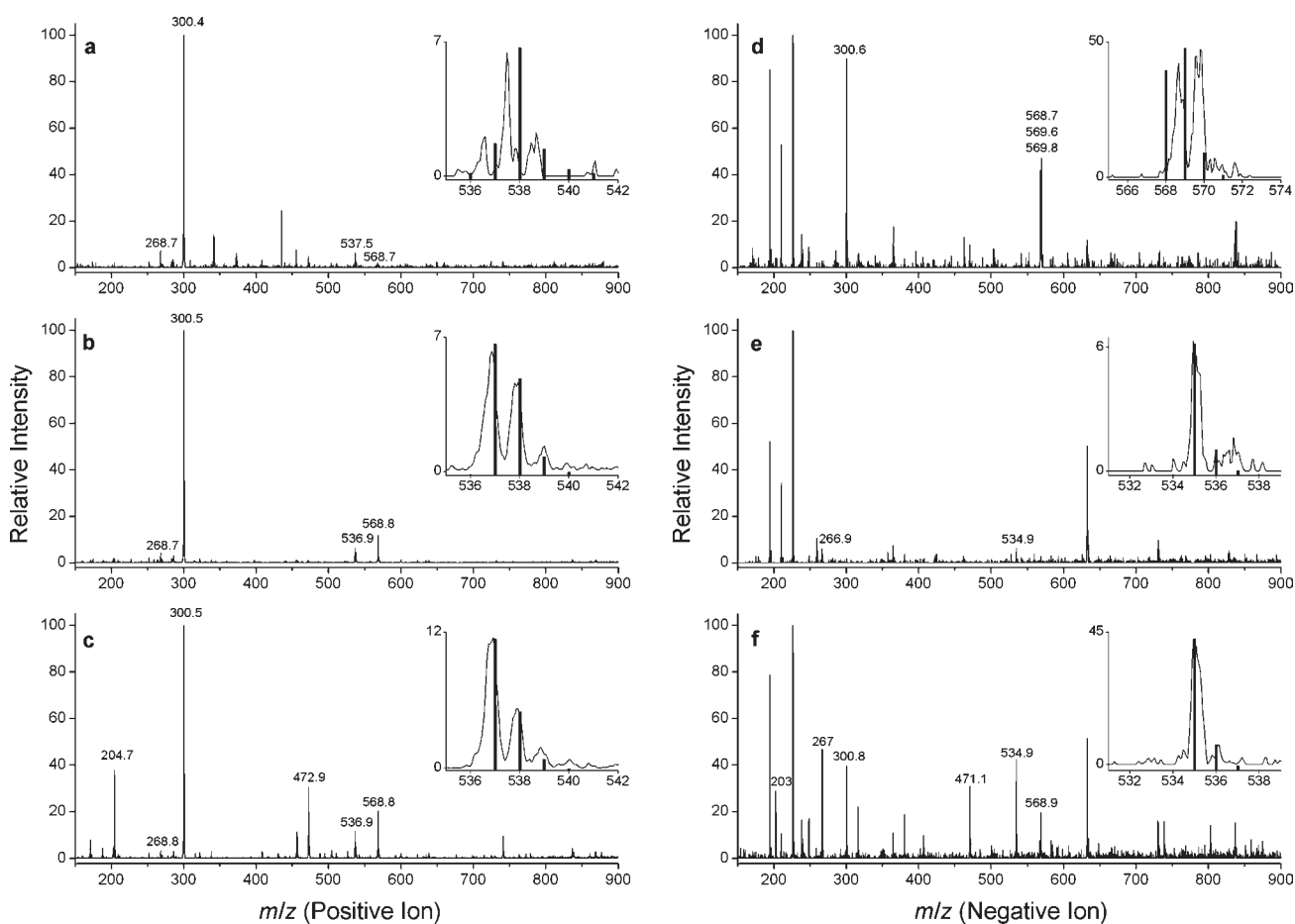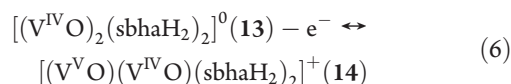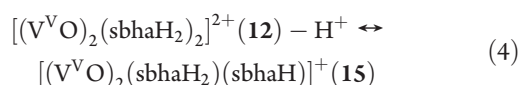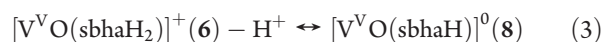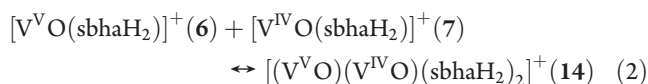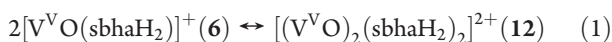
Figure 4. Positive ion ESI-MS spectra from 1:2 solutions of V(IV):sbhaH$_4$ in 1:1 H$_2$O:MeOH at: (a) pH = 2, (b) pH = 5, or (c) pH = 7. Negative ion ESI-MS spectra from 1:2 solutions of V(IV):sbhaH$_4$ in 1:1 H$_2$O:MeOH at: (d) pH = 2, (e) pH = 5, or (f) pH = 7. Simulated spectra of selected species are shown in the insets.

relatively high concentrations at pH = 2 and 7 and that intrinsically uncharged MS-inactive species were present in relatively high concentrations at pH = 5. Further, this discontinuity indicated that although the m/z values of the major signals were similar, the signal at m/z_{obs} 300.6 at pH = 2 could not be ascribed to the same species that gave the signal at m/z_{obs} 300.8 at pH = 7. The most likely explanation for the observed discontinuity was that the two species giving rise to the signals with similar m/z values varied in the oxidation state of the V center(s) and/or the protonation state of the complex.

A theoretical map of the solution equilibria of V(V)/(IV)–sbhaH$_4$ complexes (Scheme 2) shows several phenomena, including dimerization (eqs 1 and 2, refer to dotted boxes in Scheme 2), deprotonation (eqs 3 and 4), and oxidation (eqs 5 and 6). At any given pH value, these processes would yield a mixture of complexes with different charges (refer to upper horizontal bars of Scheme 2). While ESI-MS data are not an accurate reflection of equilibrium conditions, this map served to aid assigning signals to species and in providing possible pathway(s) for the formation and transformation of species.

$$2[V^VO(sbhaH_2)]^+ (\mathbf{6}) \leftrightarrow [(V^VO)_2(sbhaH_2)_2]^{2+} (\mathbf{12}) \quad (1)$$

$$[V^VO(sbhaH_2)]^+ (\mathbf{6}) + [V^{IV}O(sbhaH_2)]^+ (\mathbf{7})$$
$$\leftrightarrow [(V^VO)(V^{IV}O)(sbhaH_2)_2]^+ (\mathbf{14}) \quad (2)$$

$$[V^VO(sbhaH_2)]^+ (\mathbf{6}) - H^+ \leftrightarrow [V^VO(sbhaH)]^0 (\mathbf{8}) \quad (3)$$

$$[(V^VO)_2(sbhaH_2)_2]^{2+} (\mathbf{12}) - H^+ \leftrightarrow$$
$$[(V^VO)_2(sbhaH_2)(sbhaH)]^+ (\mathbf{15}) \quad (4)$$

$$[V^{IV}O(sbhaH_2)]^0 (\mathbf{7}) - e^- \leftrightarrow [V^VO(sbhaH_2)]^+ (\mathbf{6}) \quad (5)$$

$$[(V^{IV}O)_2(sbhaH_2)_2]^0 (\mathbf{13}) - e^- \leftrightarrow$$
$$[(V^VO)(V^{IV}O)(sbhaH_2)_2]^+ (\mathbf{14}) \quad (6)$$

ESI-MS from Solutions of V(IV) and sbhaH$_4$: Positive Ion Mode. The major signal in the positive ion ESI-MS from a 1:2 V(IV):sbhaH$_4$ solution at pH = 2 (m/z_{obs} 300.4, 100%) was ascribed to the methanol adduct $[V^VO(sbhaH_2)(CH_3OH)]^+$ (m/z_{calc} 301.1, $\mathbf{6}\cdot CH_3OH$, Scheme 2) or its dimer $[(V^VO)_2(sbhaH_2)_2(CH_3OH)_2]^{2+}$ (m/z_{calc} 301.1, $\mathbf{12}\cdot CH_3OH$, Scheme 2), which would be indistinguishable from the monomer by ESI-MS. This signal was present at 100% relative intensity from the solutions at pH = 2, 5, and 7 (Figure 4, panels a–c). Signals ascribed to the methanol free adduct $[V^VO(sbhaH_2)]^+$ (m/z_{calc} 269.1, $\mathbf{6}$) or its dimer $[(V^VO)_2(sbhaH_2)_2]^{2+}$ (m/z_{calc} 269.1, $\mathbf{12}$) were observed at lower abundance at all pH values (m/z_{obs} 268.7, 3–7%).

Scheme 2. Major Species Present in Solutions Analyzed by ESI-MS Prepared From V(IV) and sbhaH$_4$ As a Function of pH Value[a]
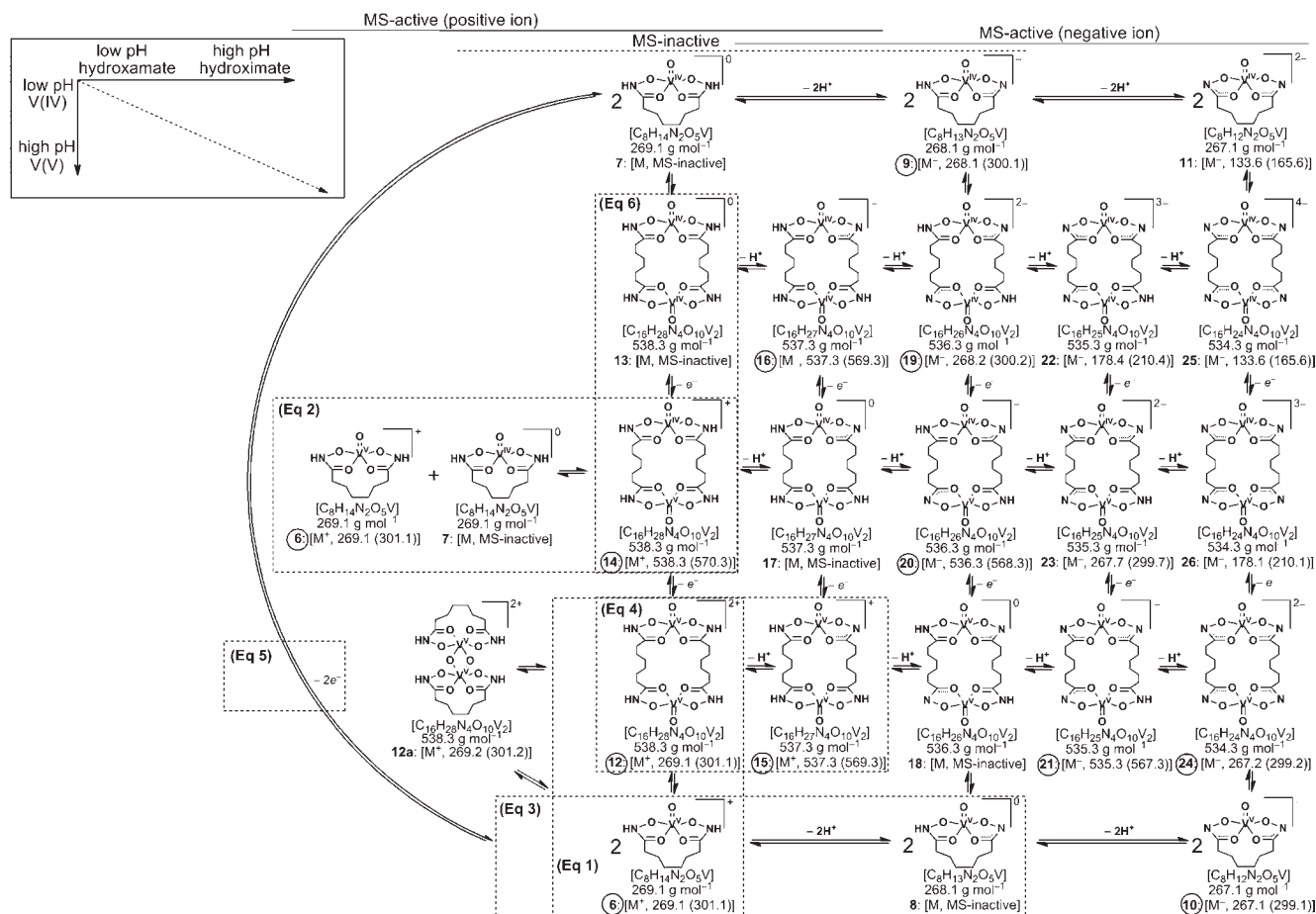
[a] The m/z_{calc} for each species is given below the structure and the m/z_{calc} value of the methanol adduct is given in parentheses.

Signals observed from the solution at pH = 5 (m/z_{obs} 536.9, 6%) and 7 (m/z_{obs} 536.9, 12%) were ascribed to $[(V^VO)_2$-$(sbhaH_2)(sbhaH)]^+$ (m/z_{calc} 537.3, **15**), which according to eq 4 could result from the single deprotonation of $[(V^VO)_2$-$(sbhaH_2)_2]^{2+}$ (**12**) or other pathways (Scheme 2). Signals observed from the solution at pH = 2 (m/z_{obs} 568.7, 2%), 5 (m/z_{obs} 568.8, 12%), and 7 (m/z_{obs} 568.8, 20%) were ascribed to the methanol adduct of **15**, $[(V^VO)_2(sbhaH_2)(sbhaH)(CH_3OH)]^+$ (m/z_{calc} 569.3, **15·CH$_3$OH**). The relative intensities of the signals ascribed to **15** and **15·CH$_3$OH** would be expected to increase with increasing pH value, which was the case. The isotope patterns of the signal from the solution at pH = 5 and 7 centered at m/z_{obs} 536.9 were not able to be simulated as a single V-sbhaH$_4$ species (Figure 4, insets in panel b and c), suggesting that the signal comprised overlapping signals from **15** and one or more other V-sbhaH$_4$ species.

The presence of the signal ascribed to **15** (m/z_{obs} 536.9) supported the existence of dimeric V-sbhaH$_4$ species. Mononuclear **6** could form dimeric **12**, in which each sbhaH$_4$ ligand bridges between two oxoV(V) centers (intermetal coordination) and dimeric **12a**, in which each sbhaH$_4$ ligand binds to discrete V(V) centers (intrametal coordination) which themselves are bound via a bis(μ-oxo) bridge. With six methylene groups separating the flanking hydroxamic acid groups, sbhaH$_4$ sits at the boundary of the preference of dihydroxamic acids with

methylene chain lengths $n \leq 6$ to form dimeric complexes (eg, **12**) and ligands with methylene chain lengths $n \geq 6$ to form mononuclear complexes (eg, **6**), as established by previous work.[49,57−60]

There was close to one m/z unit difference between a signal from the solutions at pH = 5 and 7 at m/z_{obs} 536.9 and from the solution at pH = 2 at m/z_{obs} 537.5. The difference was consistent with the presence of $[(V^VO)(V^{IV}O)(sbhaH_2)_2]^+$ (m/z_{calc} 538.2, **14**) at pH = 2 and the presence of its one-electron oxidized, single-deprotonated product **15** at pH = 5 and 7. Species **14** could arise from the dimerization of mononuclear **6** and **7** (eq 2) and/or from the one-electron oxidation of **13** (eq 6), itself a dimer of **7**. Based upon the acid stability of V(IV), the concentration of **14** would be expected to be higher at low pH and to decrease at higher pH values. Support for the presence of mixed-valence V(V)/(IV)−sbhaH$_4$ complexes at acid conditions is obtained from the crystallographically characterized mixed-valence V(V)$_2$-V(IV)-quinic acid trimer, which was isolated from a water−ethanol solution of the V(V)-quinic acid dimer upon reducing the pH value from 7.0 to 3.3.[61] Several mixed-valence V(IV)/V(V) μ-oxo-bridged complexes have been characterized with O and N donor atoms.[62−64] While the signal at m/z_{obs} 537.5 from the spectra at pH = 2 simulated reasonably well as $[(V^VO)(V^{IV}O)(sbhaH_2)_2]^+$ (**14**), an improved fit was obtained from assuming the presence of 80% $[(V^VO)(V^{IV}O)(sbhaH_2)_2]^+$

(14) and 20% $[(V^VO)_2(sbhaH_2)(sbhaH)]^+$ (15) (Figure 4, panel a, inset). The signal at m/z_{obs} 536.9 from the spectra at pH = 5 simulated as comprising 65% $[(V^VO)_2(sbhaH_2)(sbhaH)]^+$ (15) and 35% $[(V^VO)(V^{IV}O)(sbhaH_2)_2]^+$ (14) and at pH = 7 as 80% $[(V^VO)_2(sbhaH_2)(sbhaH)]^+$ (15) and 20% $[(V^VO)$-$(V^{IV}O)(sbhaH_2)_2]^+$ (14) (Figure 4). In summary, the simplest model consistent with the positive ion ESI-MS data involved the presence of monomeric or dimeric $[V^VO(sbhaH_2)]^+$ (6, 12) and the methanol adducts ($6 \cdot CH_3OH$, $12 \cdot CH_3OH$), $[(V^V)_2$-$(sbhaH_2)(sbhaH)]^+$ (15) and the methanol adduct ($15 \cdot CH_3OH$) and $[(V^VO)(V^{IV}O)(sbhaH_2)_2]^+$ (14).

ESI-MS from Solutions of V(IV) and sbhaH$_4$: Negative Ion Mode. The major signal in the negative ion ESI-MS from a 1:2 V(IV):sbhaH$_4$ solution at pH = 2 (m/z_{obs} 300.6, 90%) was ascribed to methanol adduct $[V^{IV}O(sbhaH)(CH_3OH)]^-$ (m/z_{calc} 300.1) or its dimer $[(V^{IV}O)_2(sbhaH)_2(CH_3OH)_2]^{2-}$ (m/z_{calc} 300.1) ($9 \cdot CH_3OH$ and $19 \cdot CH_3OH$, respectively, Scheme 2). This signal was absent from the solution at pH = 5 and reappeared from the solution at pH = 7, which indicated that the signals were due to different species, even though the m/z values were similar. The signal (m/z_{obs} 300.8, 20%) from the solution at pH = 7 was ascribed to the methanol adduct $[V^VO(sbha)(CH_3OH)]^-$ (m/z_{calc} 299.1) or its dimer $[(V^VO)_2$-$(sbha)_2(CH_3OH)_2]^{2-}$ (m/z_{calc} 299.1) ($10 \cdot CH_3OH$ and $24 \cdot CH_3OH$, respectively, Scheme 2). The one-electron oxidation of $[V^{IV}O(sbhaH)(CH_3OH)]^-$ ($9 \cdot CH_3OH$) would produce the MS-inactive $[V^VO(sbhaH)(CH_3OH)]^0$ ($8 \cdot CH_3OH$) consistent with the absence of a signal from the solution at pH = 5, and the deprotonation of $[V^VO(sbhaH)(CH_3OH)]^0$ ($8 \cdot CH_3OH$) would form the MS-active $[V^VO(sbha)$-$(CH_3OH)]^-$ ($10 \cdot CH_3OH$) at pH = 7. Signals ascribed to dimeric $[(V^VO)_2(sbhaH)(sbha)]^-$ (m/z_{calc} 535.3, 21) were observed from the solution at pH = 5 (m/z_{obs} 534.9, 6%) and 7 (m/z_{obs} 534.9, 42%). The isotope pattern of the signal simulated well as 21 present as a single species (Figure 4, insets in panel e and f). The relative concentration of 10, 24, and 21 would be expected to increase with increasing pH value, which was the case. The signals observed from the solution at pH = 2 (m/z_{obs} 568.7, 42% and m/z_{obs} 569.8, 47%) were ascribed to the methanol adduct of the mixed-valence dimer $[(V^VO)$-$(V^{IV}O)(sbhaH)_2(CH_3OH)]^-$ (m/z_{calc} 568.3, $20 \cdot CH_3OH$) and the methanol adduct $[(V^{IV}O)_2(sbhaH_2)(sbhaH)(CH_3OH)]^-$ (m/z_{calc} 569.3, $16 \cdot CH_3OH$), respectively. The isotope pattern in this region of the spectrum from the solution at pH = 2 indicates that $16 \cdot CH_3OH$ and $20 \cdot CH_3OH$ were present at about equal relative concentration.

ESI-MS from Solutions of V(IV) and sbhaH$_4$: Closing Comments. At any given pH value, solutions of V(IV) and shhaH$_4$ analyzed by ESI-MS showed signals that could be ascribed to monomeric or dimeric V(V)/(IV)-sbhaH$_4$ species that differed in the level of deprotonation, the oxidation state of the V center(s), and in the overall charge of the complex. In total, the presence of 11 MS-active V(V)/(IV)-sbhaH$_4$ species have been proposed (marked by circles around the species number in Scheme 2; note 6 is shown twice in eqs 1 and 2). Since three of these 11 species (12, 19, and 24) are dimers that cannot be distinguished from the respective monomers (6, 9, and 10), the minimal speciation model from ESI-MS data supported the presence of 8 species. At all pH values, the dominant species from solutions of V(IV) and sbhaH$_4$ detected in the positive ion ESI-MS was $6 \cdot CH_3OH$ and/or its dimer $12 \cdot CH_3OH$ (Figure 5). At pH = 2, a higher relative concentration of
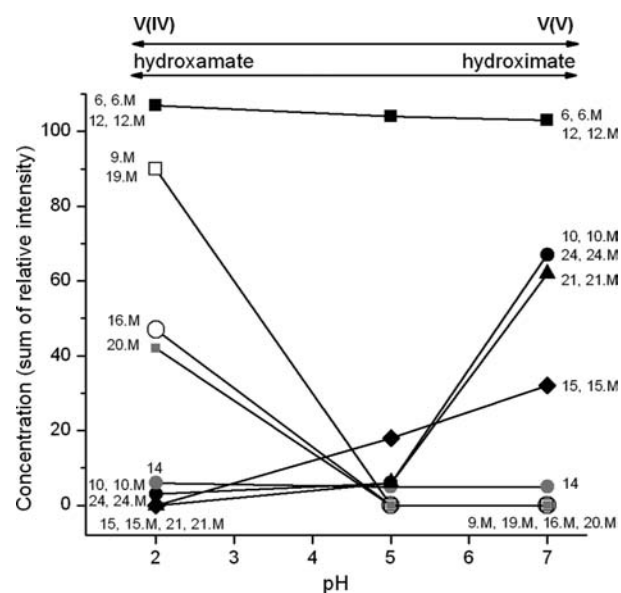

Figure 5. Distribution of species from 1:2 solutions of V(IV) and sbhaH$_4$ at pH = 2, 5, and 7, as measured by ESI-MS. V(V)-, V(IV)-, or mixed-valence V(V)/(IV)-sbhaH$_4$ species are represented by closed (black), open, or closed (gray) symbols, respectively, and by the species number, according to Scheme 2. The relative concentrations are presented as the sum of the relative intensity of the signals of a species (eg, 6) and its methanol adduct (eg, 6.M), according to Table 1.

V(IV)-sbhaH$_4$ species ($9 \cdot CH_3OH$, $19 \cdot CH_3OH$, $16 \cdot CH_3OH$) and V(IV)/(V) species (14, $20 \cdot CH_3OH$) was present, with these species not evident in significant concentrations at pH = 5 and above. The V(V)-sbhaH$_4$ species 15, $15 \cdot CH_3OH$, 10, $10 \cdot CH_3OH$, 24, $24 \cdot CH_3OH$, 21, and $21 \cdot CH_3OH$ were not evident at pH = 2 but were detectable at low levels at pH = 5 and increased in relative concentration at pH = 7 (Figure 5). The V(V)/(IV)-sbhaH$_4$ speciation profile was internally consistent across the positive and negative ion ESI-MS data. For example, the four-step deprotonation of dimeric $[(V^VO)_2(sbhaH_2)_2]^{2+}$ (m/z_{calc} 269.1; m/z_{obs} 268.7, 12) to $[(V^VO)_2(sbhaH_2)(sbhaH)]^+$ (m/z_{calc} 537.3; m/z_{obs} 536.9, 15) to $[(V^VO)_2(sbhaH)_2]^0$ (MS-inactive, 18) to $[(V^VO)_2(sbhaH)(sbha)]^-$ (m/z_{calc} 535.3; m/z_{obs} 534.9, 21) to $[(V^VO)_2(sbha)_2]^{2-}$ (m/z_{calc} 267.1; m/z_{obs} 266.9, 24) was consistent with the positive and negative ion ESI-MS data.

At higher pH values, the dominant species present in a solution prepared from V(IV) and sbhaH$_4$ tended toward the bottom right-hand region of Scheme 2. This was consistent with the increased concentrations at higher pH values of the V(V) ion and the hydroximate form of sbhaH$_4$. The V(V)/(IV)-sbhaH$_4$ speciation profile can be broadly represented as a vector sum (Scheme 2, inset, dotted vector) of a pH-dependent vector that describes the oxidation of V(IV) to V(V) (low to high pH, respectively) (Scheme 2, inset, shorter solid vector) and a pH-dependent vector that describes the deprotonation of hydroxamate to hydroximate (low to high pH, respectively) (Scheme 2, inset, longer solid vector).

^{51}V NMR Spectroscopy. A solution prepared from V(IV) and pbH$_2$ containing $[V^VO(pb)]^+$ should be detectable by ^{51}V NMR spectroscopy (V(V), d^0). The ^{51}V NMR spectrum from an approximately V(IV):pbH$_2$ = 1:1 solution at pH = 2 showed a signal at −443.3 ppm (Figure 6a), which was within the range for selected five- and six-coordinate V(V)−hydroxamato complexes
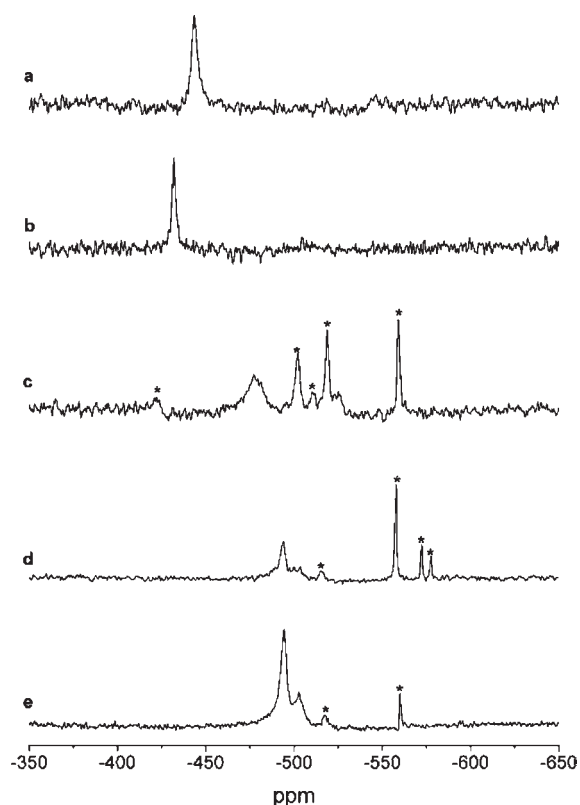
Figure 6. ^{51}V NMR spectra referenced to VOCl$_3$ (0 ppm) from a: (a) 1:1 solution of V(IV):pbH$_2$ in CD$_3$OD; 1:2 solution of V(IV):sbhaH$_4$ in D$_2$O at (b) pH = 2, (c) pH = 5, or (d) pH = 7 or a (e) 1:3 solution of V(IV): sbhaH$_4$ in D$_2$O at pH = 7. Polyoxovanadate species are denoted by *.

Figure 7. EPR spectra (150 K) from a methanol glass of: (a) VOSO$_4$· 5H$_2$O, (b) V(IV):pbH$_2$ = 1:1 (pH = 2), (c) V(IV):sbhaH$_4$ = 1:2 (pH = 2), (d) V(IV):sbhaH$_4$ = 1:2 (2 < pH < 5), and (e) V(IV):sbhaH$_4$ = 1:2 (pH = 5). Traces in black or gray are experimental or simulated spectra, respectively.

at low pH values and also other V(V) complexes with O,O′ coordination, such as diols and α-hydroxycarboxylic acids.[65−69] There were no signals attributable to polyoxovanadate species ([HVO$_4$]$^{3-}$, −557 ppm; [V$_2$O$_7$]$^{4-}$, −571 ppm; [V$_4$O$_{12}$]$^{4-}$,−577 ppm) in the spectrum[70] which suggested that the signal was attributable to [V^{V}O(pb)]$^+$ or [V^{V}O(OH)(pb)].

A signal in the ^{51}V NMR spectrum at −432.2 ppm from a 1:2 solution of V(IV):sbhaH$_4$ at pH = 2 suggested the presence of a single V(V)-sbhaH$_4$ species (Figure 6b). This is consistent with the posit that there exists a mixture of V(IV)-sbhaH$_4$ and V(V)-sbhaH$_4$ species in a solution prepared from V(IV) and sbhaH$_4$ at pH = 2. Similar to the case with pbH$_2$, there were no signals due to polyoxovanadate species at this pH value. The signal at −432 ppm was absent from V(IV):sbhaH$_4$ = 1:2 solutions at pH = 5 (Figure 6c) and 7 (Figure 6d) with broad signals ascribed to V(V)−sbhaH$_4$ complexes appearing at −478 or −493 ppm, at the respective pH values. The relative intensity of the signal at −493 ppm increased at V(IV):sbhaH$_4$ = 1:3, pH = 7 (Figure 6e). The significant upfield shift of these signals from −432.2 ppm at pH = 2 indicated the formation of different V(V)-sbhaH$_4$ species, possibly arising from a mixture of hydroxamate- and hydroximate-coordination modes. At pH = 5 and 7, signals due to polyoxovanadate species ([V$_{10}$O$_{28}$]$^{6-}$, [H$_2$V$_{10}$O$_{28}$]$^{4-}$, [HVO$_4$]$^{2-}$, [V$_2$O$_7$]$^{4-}$, [V$_4$O$_{12}$]$^{4-}$) were evident (signals marked with * in Figure 6).

EPR Spectroscopy. If [V^{V}O(pb)]$^+$ was the dominant species formed from solutions of V(IV) and pbH$_2$, then these solutions would be expected to be EPR silent. Compared to the EPR signal (150 K) from a methanol glassy solution of VOSO$_4$ (10 mM,
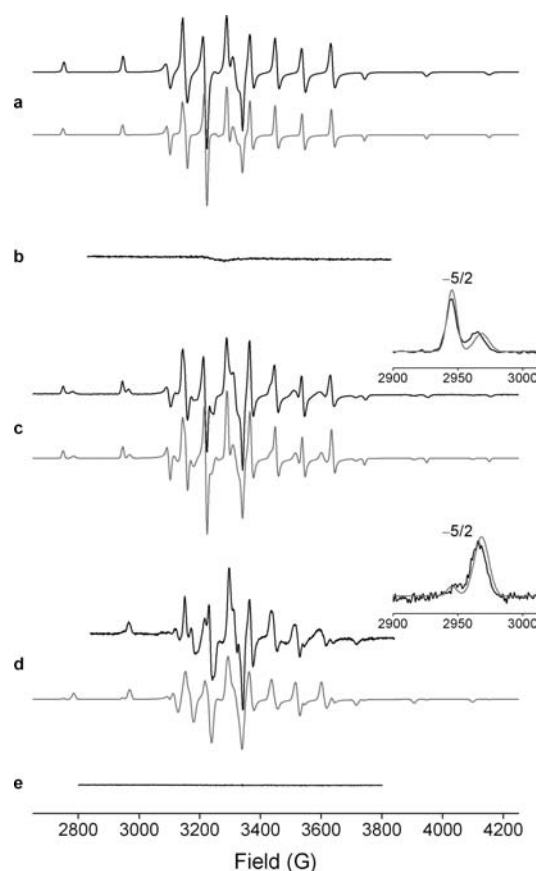
Figure 7a), there was no signal in the EPR spectrum from a methanol glassy solution of V(IV) and pbH$_2$ at pH = 2 (Figure 7b), which supports the notion that these solutions contained [V^{V}O(pb)]$^+$. The calculated EPR parameters from the VOSO$_4$ spectrum as simulated using QPOW[71] ($g_{\parallel}$ = 1.933, $A_{\parallel}$ = 181.2 × 10^{-4} cm^{-1}; $g_{\perp}$ = 1.976, $A_{\perp}$ = 70.7 × 10^{-4} cm^{-1}) agreed well with literature values for VOSO$_4$ ($g_{\parallel}$ = 1.933, $A_{\parallel}$ = 183 × 10^{-4} cm^{-1}; $g_{\perp}$ = 1.978, $A_{\perp}$ = 71 × 10^{-4} cm^{-1}).[72,73] A methanol glassy solution of V(IV) and sbhaH$_4$ at approximately pH = 2 gave an EPR signal (Figure 7c) that indicated the presence of more than one species, which was more clearly evident from the signal at the −5/2 resonance (inset). It was reasonable to assume that this solution contained a mixture of VOSO$_4$ and V(IV)-sbhaH$_4$ species. Therefore, while solutions of V(IV) and pbH$_2$ exclusively yielded V(V)-pbH$_2$ species, solutions of V(IV) and sbhaH$_4$ yielded a mixture of V(IV)-sbhaH$_4$ species, as evidenced from the EPR spectroscopic data, and V(V)-sbhaH$_4$ species, as evidenced from the ^{51}V NMR spectroscopic and electronic absorption spectroscopic data. This was also consistent with the distribution of V(V)- and V(IV)-sbhaH$_4$ species detected by ESI-MS (Table 1, Figure 5). A second spectrum was acquired from a different solution prepared from VOSO$_4$ and sbhaH$_4$ with the pH value approximately at pH = 2 (Figure 7d) which indicated the presence of VOSO$_4$ and V(IV)-sbhaH$_4$ species in different relative concentrations to Figure 7c
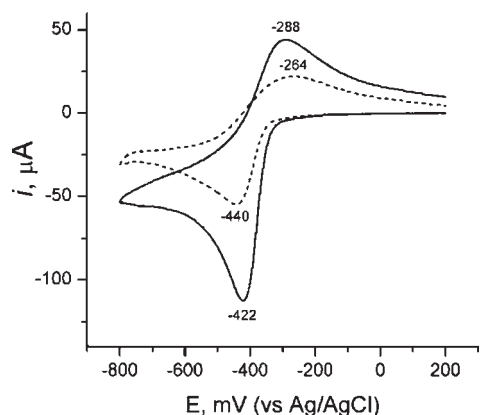
Figure 8. Cyclic voltammograms from solutions of $[V(IV)]:[pbH_2] =$ 1:1 (solid line) or $[V(IV)]:[sbhaH_4] =$ 1:2 (dashed line) in 0.1 M NaCl at pH = 2.

(refer to −5/2 resonance in inset). The solution from Figure 7d contained a higher relative concentration of V(IV)-sbhaH$_4$ species and enabled the calculation of the EPR parameters of the V(IV)-sbhaH$_4$ species as: $g_\parallel$ = 1.939, $A_\parallel$ = 170.1 × 10^{-4} cm^{-1}; $g_\perp$ = 1.979, $A_\perp$ = 63.4 × 10^{-4} cm^{-1}. The values of the line widths at half height for the V(IV)-sbhaH$_4$ species ($W_\perp$ = 8.0 × 10^{-4} cm^{-1}; $W_\parallel$ = 6.0 × 10^{-4} cm^{-1}) were almost twice the values for VOSO$_4$ ($W_\perp$ = 5.0 × 10^{-4} cm^{-1}; $W_\parallel$ = 4.0 × 10^{-4} cm^{-1}), which suggested that more than one V(IV)-sbhaH$_4$ species was present. The most likely species to be attributed to the V(IV)-sbhaH$_4$ EPR signal were **9·**CH$_3$OH, **19·**CH$_3$OH, or **16·**CH$_3$OH, since these were present in relatively high concentration according to the ESI-MS data. The relative concentrations of VOSO$_4$ and V(IV)-sbhaH$_4$ species in the solution from Figure 7c were 70:30 and in the solution from Figure 7d were 10:90. The increased signal-to-noise of the spectra in Figure 7d compared to Figure 7c indicated that the total concentration of V(IV) species in the solution from Figure 7d was less than that in Figure 7c. An EPR spectrum from a solution of VOSO$_4$ and sbhaH$_4$ at pH = 5 was EPR silent (Figure 7e). Therefore, the pH value of the solution in Figure 7d was likely to have been above pH = 2. The higher relative concentration of EPR silent V(V)-sbhaH$_4$ species at pH values >5 was consistent with the V(V)/(IV)-sbhaH$_4$ speciation model from the ESI-MS data.

Cyclic Voltammetry. As supported by data from ESI-MS and ^{51}V NMR spectroscopy, the major species present in a solution of V(IV) and pbH$_2$ were due to $[V^VO(pb)]^+$ or its dimer. The absence of a signal in the EPR spectrum from these solutions suggested that the concentration of V(IV) species was negligible. Analogous studies with the linear dihydroxamic acid sbhaH$_4$ showed a distribution of monomeric and dimeric V(IV) and V(V) species and mixed-valence V(V)/(IV) species. These results indicated that the thermodynamic stability of a complex formed between V(V) and the macrocyclic dihydroxamic acid pbH$_2$ would be greater than that with the linear dihydroxamic acid, which suggested that the V(V)/(IV) redox potential of $[V^VO(pb)]^+$ would be less than that of the V-sbhaH$_4$ system. Cyclic voltammetry from a 1:1 solution of V(IV):pbH$_2$ at pH = 2 (Figure 8) showed a reversible reduction with a half-wave potential $E_{1/2}$ = −335 mV (Figure 8, solid line). The half-wave potential of the cyclic voltammogram from a 1:2 solution of V(IV):sbhaH$_4$ at pH = 2 was $E_{1/2}$ = −352 mV (Figure 8, dashed line). This was the opposite of what was predicted based on the

solution speciation results ($E_{1/2}$ $[VO(pb)]^{+/0}$ < $V^{V/IV}$-sbhaH$_4$). The difference of 17 mV in the half-wave potential is rather small. Second, while a 1:1 solution of V(IV):pbH$_2$ at pH = 2 yielded $[V^VO(pb)]^+$, the 1:2 solution of V(IV):sbhaH$_4$ at pH = 2 contained at a minimum VOSO$_4$ and a mixture of V(V)-sbhaH$_4$, V(IV)-sbhaH$_4$, and V(V)/(IV)-sbhaH$_4$ species (Table 1), which would prevent the determination of the half-wave potential of a unique species.

CONCLUDING REMARKS

Multiple spectroscopic methods have shown that the monooxoV(V) complex $[V^VO(pb)]^+$ was the dominant species formed from solutions of V(IV) and the cyclic dihydroxamic acid pbH$_2$. As predicted, the cyclic dihydroxamic acid is suitably preorganized for oxoV(V) coordination. The characterization of $[V^VO(pb)]^+$ expands the small family of V−siderophore complexes that have been described. Solutions of V(IV) and the linear dihydroxamic acid sbhaH$_4$ gave mixtures with higher relative concentrations of hydroxamate-based V(IV)-sbhaH$_4$, V(IV)/V(V)-sbhaH$_4$, and V(V)-sbhaH$_4$ species at pH = 2 and higher concentrations of hydroximate-based V(V)-sbhaH$_4$ species at pH = 7. The complexity of the V-sbhaH$_4$ solution equilibria arose from phenomena including dimerization ($2[V^VO(sbhaH_2)]^+ \leftrightarrow [(V^VO)_2(sbhaH_2)_2]^{2+}$), deprotonation ($[V^VO(sbhaH_2)]^+ - H^+ \leftrightarrow [V^VO(sbhaH)]^0$), and oxidation ($[V^{IV}O(sbhaH_2)]^0 - e^- \leftrightarrow [V^VO(sbhaH_2)]^+$) and can be described as the sum of two pH-dependent vectors, the first comprising the deprotonation of hydroxamate to hydroximate (low to high pH, respectively) and the second comprising the oxidation of V(IV) to V(V) (low to high pH, respectively).

The restricted conformational freedom of pbH$_2$ compared to linear sbhaH$_4$ likely accounts for the entropic-based increase in the thermodynamic stability of $[V^VO(pb)]^+$ compared to that of the V-sbhaH$_4$ species. The preorganization of metal binding functional groups in macrocyclic peptides manifests as greater selectivity and stronger binding compared to their linear analogues[74,75] and is reflected in the greater stability of Fe(III) complexes of cyclic hydroxamic acid-based siderophores, such as alcaligin ($1/2\log\beta_{230}$ = 32.4) and desferrioxamine E ($\log\beta_{110}$ = 32.5), compared to linear siderophores, such as desferrioxamine B ($\log\beta_{110}$ = 30.5).[76,77] The stability of $[V^VO(pb)]^+$ suggested to us that the oxoV(V) ion could be used to preorganize the assembly of two endohydroxamic acid amino carboxylic acid units prior to end-to-end peptide-based cyclization to furnish $[V^VO(pb)]^+$. We will shortly publish our results of the V(V)-based templated synthesis of $[V^VO(pb)]^+$ and new cyclic dihydroxamic acids.

Each of pbH$_2$ and the related bisucaberin are siderophores native to marine bacteria, including species of the genus *Shewanella*. The formation of $[V^VO(pb)]^+$ at pH values 2−7 is relevant in the context of the competition between pbH$_2$ and Fe(III) or V(V) in surface oxic marine waters and provides knowledge of the ligands potentially involved in V acquisition and uptake, so-called 'vanadophores', in microorganisms and other forms of life.[20]

ASSOCIATED CONTENT

ⓢ Supporting Information. Positive and negative ion mode ESI-MS data from 1:2 solutions of V(IV):sbhaH$_4$ at pH = 2, 5, 7, and 9 and from 1:1 solutions of V(IV):sbhaH$_4$ at

pH = 2 (positive ion mode). This material is available free of charge via the Internet at http://pubs.acs.org.

■ AUTHOR INFORMATION

Corresponding Author

*E-mail: rachel.codd@sydney.edu.au. Telephone +61 (0)2 9351-6738.

■ REFERENCES

(1) Budzikiewicz, H. In *Progress in the Chemistry of Organic Natural Products*; Kinghorn, A. D., Falk, H., Kobayashi, J., Eds.; Springer-Verlag: New York, 2010; Vol. 92, p 1−75.

(2) Hider, R. C.; Kong, X. *Nat. Prod. Rep.* 2010, 27, 637−657.

(3) Miller, M. J.; Zhu, H.; Xu, Y.; Wu, C.; Walz, A. J.; Vergne, A.; Roosenberg, J. M.; Moraski, G.; Minnick, A. A.; McKee-Dolence, J.; Hu, J.; Fennell, K.; Dolence, E. K.; Dong, L.; Franzblau, S.; Malouin, F.; Mollmann, U. *BioMetals* 2009, 22, 61−75.

(4) Butler, A.; Theisen, R. M. *Coord. Chem. Rev.* 2010, 254, 288−296.

(5) Sandy, M.; Butler, A. *Chem. Rev.* 2009, 109, 4580−4595.

(6) Butler, A. *BioMetals* 2005, 18, 369−374.

(7) Crumbliss, A. L.; Harrington, J. M. *Adv. Inorg. Chem.* 2009, 61, 179−250.

(8) Braun, V.; Hantke, K. In *Microbial Transport Systems*; Winkelmann, G., Ed.; Wiley-VCH: Weinheim, Germany, 2002, p 289−311.

(9) Miethke, M.; Marahiel, M. A. *Microbiol. Mol. Biol. Rev.* 2007, 71, 413−451.

(10) Winkelmann, G. *Biochem. Soc. Trans.* 2002, 30, 691−696.

(11) Raymond, K. N.; Dertz, E. A. In *Iron Transport in Bacteria*; Crosa, J. H., Mey, A. R., Payne, S. M., Eds.; ASM Press: Washington, DC, 2004, p 3−17.

(12) Boukhalfa, H.; Crumbliss, A. L. *BioMetals* 2002, 15, 325−339.

(13) Drechsel, H.; Winkelmann, G. In *Transition Metals in Microbial Metabolism*; Winkelmann, G., Carrano, C. J., Eds.; Harwood Academic: Amsterdam, The Netherlands, 1997, p 1−49.

(14) Marmion, C. J.; Griffith, D.; Nolan, K. B. *Eur. J. Inorg. Chem.* 2004, 3003−3016.

(15) Liu, J.; Obando, D.; Schipanski, L. G.; Groebler, L. K.; Witting, P. K.; Kalinowski, D. S.; Richardson, D. R.; Codd, R. *J. Med. Chem.* 2010, 53, 1370−1382.

(16) Codd, R.; Braich, N.; Liu, J.; Soe, C. Z.; Pakchung, A. A. H. *Int. J. Biochem. Cell Biol.* 2009, 41, 736−739.

(17) Braich, N.; Codd, R. *Analyst* 2008, 133, 877−880.

(18) Minucci, S.; Pelicci, P. G. *Nat. Rev. Cancer* 2006, 6, 38−51.

(19) Codd, R. *Coord. Chem. Rev.* 2008, 252, 1387−1408.

(20) Rehder, D. *Org. Biomol. Chem.* 2008, 6, 957−964.

(21) Bellenger, J. P.; Wichard, T.; Kraepiel, A. M. L. *Appl. Environ. Microbiol.* 2008, 74, 1478−1484.

(22) Butler, A.; Parsons, S. M.; Yamagata, S. K.; de la Rosa, R. I. *Inorg. Chim. Acta* 1989, 163, 1−3.

(23) Bell, J. H.; Pratt, R. F. *Biochemistry* 2002, 41, 4329−4338.

(24) Goldwaser, I.; Li, J.; Gershonov, E.; Armoni, M.; Karnieli, E.; Fridkin, M.; Shechter, Y. *J. Biol. Chem.* 1999, 274, 26617−26624.

(25) Haratake, M.; Fukunaga, M.; Ono, M.; Nakayama, M. *J. Biol. Inorg. Chem.* 2005, 10, 250−258.

(26) Karpishin, T. B.; Raymond, K. N. *Angew. Chem., Int. Ed. Engl.* 1992, 31, 466−468.

(27) Karpishin, T. B.; Dewey, T. M.; Raymond, K. N. *J. Am. Chem. Soc.* 1993, 115, 1842−1851.

(28) Luterotti, S.; Grdinic, V. *Analyst* 1986, 111, 1163−1165.

(29) Ledyard, K. M.; Butler, A. *J. Biol. Inorg. Chem.* 1997, 2, 93−97.

(30) Kadi, N.; Arbache, S.; Song, L.; Oves-Costales, D.; Challis, G. L. *J. Am. Chem. Soc.* 2008, 130, 10458−10459.

(31) Gram, L. *Appl. Environ. Microbiol.* 1994, 60, 2132−2136.

(32) Brickman, T. J.; Anderson, M. T.; Armstrong, S. K. *BioMetals* 2007, 20, 303−322.

(33) Nishio, T.; Tanaka, N.; Hiratake, J.; Katsube, Y.; Ishida, Y.; Oda, J. *J. Am. Chem. Soc.* 1988, 110, 8733−8734.

(34) Kameyama, T.; Takahashi, A.; Kurasawa, S.; Ishizuka, M.; Okami, Y.; Takeuchi, T.; Umezawa, H. *J. Antibiot.* 1987, 40, 1664−1670.

(35) Kadi, N.; Song, L.; Challis, G. L. *Chem. Commun.* 2008, 5119−5121.

(36) Hou, Z.; Sunderland, C. J.; Nishio, T.; Raymond, K. N. *J. Am. Chem. Soc.* 1996, 118, 5148−5149.

(37) Carrano, C. J.; Raymond, K. N. *J. Am. Chem. Soc.* 1978, 100, 5371−5374.

(38) Boukhalfa, H.; Brickman, T. J.; Armstrong, S. K.; Crumbliss, A. L. *Inorg. Chem.* 2000, 39, 5591−5602.

(39) Bergeron, R. J.; McManis, J. S. *Tetrahedron* 1989, 45, 4939−4944.

(40) Bergeron, R. J.; McManis, J. S.; Perumal, P. T.; Algee, S. E. *J. Org. Chem.* 1991, 56, 5560−5563.

(41) Fisher, D. C.; Barclay-Peet, S. J.; Balfe, C. A.; Raymond, K. N. *Inorg. Chem.* 1989, 28, 4399−4406.

(42) Gez, S.; Luxenhofer, R.; Levina, A.; Codd, R.; Lay, P. A. *Inorg. Chem.* 2005, 44, 2934−2943.

(43) Pakchung, A. A. H.; Soe, C. Z.; Codd, R. *Chem. Biodivers.* 2008, 5, 2113−2123.

(44) Simpson, P. J. L.; Richardson, D. J.; Codd, R. *Microbiology* 2010, 156, 302−312.

(45) Butler, A. *Science* 1998, 281, 207−210.

(46) Abbasi, S. *Anal. Chem.* 1976, 48, 714−717.

(47) Pande, K. R.; Tandon, S. G. *J. Inorg. Nucl. Chem.* 1980, 42, 1509.

(48) Monga, V.; Thompson, K. H.; Yuen, V. G.; Sharma, V.; Patrick, B. O.; McNeill, J. H.; Orvig, C. *Inorg. Chem.* 2005, 44, 2678−2688.

(49) Spasojevic, I.; Boukhalfa, H.; Stevens, R. D.; Crumbliss, A. L. *Inorg. Chem.* 2001, 40, 49−58.

(50) Pecoraro, V. L. *Inorg. Chim. Acta* 1989, 155, 171−173.

(51) Brown, D. A.; Glass, W. K.; Mageswaran, R.; Girmay, B. *Magn. Reson. Chem.* 1988, 26, 970−973.

(52) Brown, D. A.; Glass, W. K.; Mageswaran, R.; Mohanmmed, S. A. *Magn. Reson. Chem.* 1991, 29, 40−45.

(53) Brown, D. A.; Coogan, R. A.; Fitzpatrick, N. J.; Glass, W. K.; Abukshima, D. E.; Shiels, L.; Ahlgrén, M.; Smolander, K.; Pakkanen, T. T.; A., P. T.; Peräkylä, M. *J. Chem. Soc., Perkins Trans. 2* 1996, 2673−2679.

(54) Schraml, J.; Kvícalová, M.; Blechta, V.; Soukupová, L.; Exner, O.; Boldhaus, H.-M.; Erdt, F.; Bliefert, C. *Magn. Reson. Chem.* 2000, 38, 795−801.

(55) Kakkar, R.; Grover, R.; Chadha, P. *Org. Biomol. Chem.* 2003, 1, 2200−2206.

(56) Comiskey, J.; Farkas, E.; Krot-Lacina, K. A.; Pritchard, R. R.; McAuliffe, C. A.; Nolan, K. B. *Dalton Trans.* 2003, 4243−4249.

(57) Evers, A.; Hancock, R. D.; Martell, A. E.; Motekaitis, R. J. *Inorg. Chem.* 1989, 28, 2189−2195.

(58) Caudle, M. T.; Cogswell, L. P. I.; Crumbliss, A. L. *Inorg. Chem.* 1994, 33, 4759−4773.

(59) Farkas, E.; Bátka, D.; Pataki, Z.; Buglyó, P.; Santos, M. A. *Dalton Trans.* 2004, 1248−1253.

(60) Brown, D. A.; Geraty, R.; Glennon, J. D.; Choileain, N. N. *Inorg. Chem.* 1986, 25, 3792−3796.

(61) Codd, R.; Hambley, T. W.; Lay, P. A. *Inorg. Chem.* 1995, 34, 877−882.

(62) Huang, X.-H.; Huang, C.-C.; Qin, X.-H.; Zhai, L.-S.; Liu, D.-S. *Inorg. Chem. Commun.* **2008**, *11*, 1236–1238.

(63) Chen, C.-Y.; Zhou, Z.-H.; Chen, H.-B.; Huang, P.-Q.; Tsai, K.-R.; Chow, Y. L. *Inorg. Chem.* **2008**, *47*, 8714–8720.

(64) Jin, Y.; Lee, H.-I.; Pyo, M.; Lah, M. S. *Dalton Trans.* **2005**, 797–803.

(65) Rehder, D.; Weidemann, C.; Duch, A.; Priebsch, W. *Inorg. Chem.* **1988**, *27*, 584–587.

(66) Crans, D. C.; Felty, R. A.; Chen, H.; Eckert, H.; Das, N. *Inorg. Chem.* **1994**, *33*, 2427–2438.

(67) Hati, S.; Batchelor, R. J.; Einstein, F. W. B.; Tracey, A. S. *Inorg. Chem.* **2001**, *40*, 6258–6265.

(68) Yamaki, R. T.; Paniago, E. B.; Carvalho, S.; Lula, I. S. *J. Chem. Soc., Dalton Trans.* **1999**, 4407–4412.

(69) Jiang, F.; Anderson, O. P.; Miller, S. M.; Chen, J.; Mahroof-Tahir, M.; Crans, D. C. *Inorg. Chem.* **1998**, *37*, 5439–5451.

(70) Rehder, D. In *Transition Metal Nuclear Magnetic Resonance*; Pregosin, P. S., Ed.; Elsevier: Amsterdam, The Netherlands, 1991, p 1−58.

(71) Nilges, M. J. PhD Thesis, University of Illinois: Champaign, IL, 1979.

(72) Albanese, N. F.; Chasteen, N. D. *J. Phys. Chem.* **1978**, *82*, 910–914.

(73) Chasteen, N. D. In *Biological Magnetic Resonance*; Berliner, L. J. R., J., Ed.; Plenum Press: New York, 1981; Vol. 3, p 53−119.

(74) McGeary, R. P.; Fairlie, D. P. *Curr. Opin. Drug Discovery Dev.* **1998**, *1*, 208–217.

(75) Driggers, E. M.; Hale, S. P.; Lee, J.; Terrett, N. K. *Nat. Rev. Drug Discovery* **2008**, *7*, 608–624.

(76) Hou, Z.; Raymond, K. N.; O'Sullivan, B.; Esker, T. W.; Nishio, T. *Inorg. Chem.* **1998**, *37*, 6630–6637.

(77) Spasojevic, I.; Armstrong, S. K.; Brickman, T. J.; Crumbliss, A. L. *Inorg. Chem.* **1999**, *38*, 449–454.